

Tuning the Ionicity of Stable Metal-Organic Frameworks through Ionic Linker Installation

Jiandong Pang, Shuai Yuan, Jun-Sheng Qin, Christina Lollar, Ning Huang, Jialuo Li, Qi Wang, Mingyan Wu, Daqiang Yuan, Maochun Hong, and Hong-Cai Zhou

J. Am. Chem. Soc., **Just Accepted Manuscript** • DOI: 10.1021/jacs.8b12530 • Publication Date (Web): 28 Jan 2019

Downloaded from <http://pubs.acs.org> on January 28, 2019

Just Accepted

“Just Accepted” manuscripts have been peer-reviewed and accepted for publication. They are posted online prior to technical editing, formatting for publication and author proofing. The American Chemical Society provides “Just Accepted” as a service to the research community to expedite the dissemination of scientific material as soon as possible after acceptance. “Just Accepted” manuscripts appear in full in PDF format accompanied by an HTML abstract. “Just Accepted” manuscripts have been fully peer reviewed, but should not be considered the official version of record. They are citable by the Digital Object Identifier (DOI®). “Just Accepted” is an optional service offered to authors. Therefore, the “Just Accepted” Web site may not include all articles that will be published in the journal. After a manuscript is technically edited and formatted, it will be removed from the “Just Accepted” Web site and published as an ASAP article. Note that technical editing may introduce minor changes to the manuscript text and/or graphics which could affect content, and all legal disclaimers and ethical guidelines that apply to the journal pertain. ACS cannot be held responsible for errors or consequences arising from the use of information contained in these “Just Accepted” manuscripts.



Tuning the Ionicity of Stable Metal-Organic Frameworks through Ionic Linker Installation

Jiandong Pang,^{†,#} Shuai Yuan,^{†,#} Jun-Sheng Qin,[†] Christina T. Lollar,[†] Ning Huang,[†] Jialuo Li,[†] Qi Wang,[†] Mingyan Wu,^{‡,§} Daqiang Yuan,^{*,‡,§} Maochun Hong,^{‡,§} and Hong-Cai Zhou^{*,†}

[†]Department of Chemistry, Texas A&M University, College Station, Texas 77843-3255, United States

[‡]State Key Laboratory of Structure Chemistry, Fujian Institute of Research on the Structure of Matter, Chinese Academy of Sciences, Fuzhou, Fujian 350002, China

[§]University of Chinese Academy of Sciences, Beijing 100049, China

Supporting Information Placeholder

ABSTRACT: The predictable topologies and designable structures of metal-organic frameworks (MOFs) are the most important advantages for this emerging crystalline material compared to traditional porous materials. However, pore-environment engineering in MOF materials is still a huge challenge when it comes to the growing requirements of expanded applications. A useful method for the regulation of pore-environments, linker installation, has been developed and applied to a series of microporous MOFs. Herein, employing PCN-700 and PCN-608 as platforms, ionic linker installation was successfully implemented in both microporous and mesoporous Zr-based MOFs to afford a series of ionic frameworks. Selective ionic dye capture results support the ionic nature of these MOFs. The mesopores in PCN-608 are able to survive after installation of the ionic linkers, which is useful for ion exchange and further catalysis. To illustrate this, Ru(bpy)₃²⁺, a commonly used photoactive cation, was encapsulated into the anionic mesoporous PCN-608-SBDC *via* ion exchange. Photocatalytic activity of Ru(bpy)₃@PCN-608-SBDC was examined by aza-Henry reactions, which show good catalytic performance over three catalytic cycles.

INTRODUCTION

Metal-organic frameworks (MOFs), also known as porous coordination polymers (PCPs), have attracted considerable research attention owing to their unlimited structural diversity and functional tunability.¹⁻⁴ Indeed, the pore environment of MOFs can be precisely designed with atomic precision, leading to numerous advances in basic sciences and applications including gas storage, separation, ion exchange, chemical sensing, catalysis, energy harvesting, and biomedicine.⁵⁻¹⁷ MOF structures are formed by connecting metal-containing nodes with organic linkers through coordination bonds. The positive charges of the metal cations are usually compensated by the negatively charged organic linkers forming an electrically neutral framework.¹⁸ By virtue of the high tunability of framework fragments, ionic MOFs may be realized through residual charges on the framework and counterions in the cavity. Ionic MOFs represent a unique class of MOF materials that combines inherent porosity, structural tunability, and ion exchange capability. They have been explored as potential alternatives to conventional ion exchangers for various applications including ion separation, water purification, etc.¹⁹⁻²⁴

To construct ionic MOFs, one of two main strategies are adopted. First, ionic MOFs can be constructed from utilization of charged metal clusters as inorganic building units. For example, Feng and coworkers have constructed a series of cationic MOFs based on positively charged In₃O(COO)₆⁺ clusters.²⁵⁻²⁷ Secondly, extra charges can be introduced onto the organic linkers by -SO₃⁻ or -NR₃⁺ groups, which alter the

iconicity of the whole framework. A representative example is IRMOF-76, a cationic MOF possessing imidazolium moieties (NHC precursors) on each linker.²⁸

Compared with the myriad of neutral MOFs in the literature, the field of ionic MOFs is less explored possibly due to synthetic difficulties.²⁹ Indeed, there have been a limited number of charged metal clusters that are suitable for MOF synthesis. Employment of organic linkers with extra charge may often lead to unexpected framework structures during self-assembly. In addition, some charged functional groups, such as -NR₃⁺, cannot survive harsh solvothermal synthesis conditions. Moreover, counterion exchange might occur, whereby free Na⁺ is replaced with strongly coordinating transition metals, thus deactivating the -SO₃Na⁺ groups. Amongst the scarce number of ionic MOFs, many of them exhibit limited chemical stability. This hinders the practicality of ionic MOFs because acidic or basic conditions are usually required for material regeneration after ion exchange. Compared with the well-established synthetic methods for neutral MOFs, a general method to simultaneously control the structure, stability, and ionicity of MOFs is still lacking. This synthetic difficulty is attributed to an inherent lack of MOF formation control in one-pot reactions.

Recently, our group developed a stepwise synthetic method, namely linker installation, to introduce functional groups into stable MOFs under mild conditions.³⁰ In this method, Zr-MOFs with coordinatively unsaturated Zr₆O₄(OH)₈(H₂O)₄ clusters are selected as matrices. Linear dicarboxylate linkers with specific functional groups are subsequently installed into the matrices by occupying the coordination vacancies on the

$Zr_6O_4(OH)_8(H_2O)_4$ clusters.³¹⁻³³ Herein, we propose that linkers with designated ionic functional groups can be installed into stable Zr-MOFs to tune the ionicity of the whole structure without altering the pore size or stability. Using this method, cationic and anionic moieties were incorporated into a series of microporous and mesoporous MOFs. The resulting cationic and anionic Zr-MOFs represents a combination of high chemical stability, tunable porosity, and adjustable ionicity.

RESULTS AND DISCUSSION

Selection of the MOF Platforms. Our group has previously confirmed PCN-700 as a good microporous MOF candidate for linker installation.³¹ Besides the coordinatively-unsaturated Zr_6 clusters, the inherent flexibility of PCN-700 also plays an important role in the process of linker installation. Therefore, a mesoporous Zr-MOF with both 8-connected Zr_6 clusters and intrinsic flexibility makes for a perfect platform to apply this strategy. In addition to PCN-700, we have also constructed a series of similar microporous Zr-MOFs based on tetratopic carboxylate ligands, *i.e.* the PCN-605, PCN-606, and PCN-609 series, which also show significant flexibility due to the rotation and deformation of the ligands.³³⁻³⁵ Multi-step linker installation has been especially successful in the **scu** topology PCN-606 and PCN-609 series to afford several quaternary or quinary multivariate MOFs. Luckily, the PCN-608 series, a class of mesoporous MOFs that are topologically similar to

PCN-222 and NU-1000, can also be obtained utilizing C_{2v} symmetry, tetratopic carboxylate ligands which are also based on coordinatively unsaturated 8-connected Zr_6 clusters. Furthermore, a similar open pocket can be observed in PCN-608 with a size of approximately 8.2 Å, which is expected to fit a BDC ligand (Figure S7). Therefore, PCN-608 was selected as the mesoporous prototype MOF for installation of the ionic linkers.

Tuning the Ionicity of MOFs by Linker Installation.

Constructed by the linear Me_2 -BPDC ligand (2,2'-dimethylbiphenyl-4,4'-dicarboxylic acid) and Zr_6 cluster, PCN-700 can be considered a structural derivative of the famous UiO-67 with four linkers in the equatorial plane of the octahedral secondary building unit eliminated (Figure 1a & 1e). Therefore, the topology of PCN-700 was changed to a 8-c **bcu** network from that of a 12-c **fcu** framework with a decrease in the connection number of the Zr_6 cluster. As has been confirmed in our previous work, an H_2 BDC (1,4-benzenedicarboxylic acid) ligand can be post-synthetically installed into PCN-700 and connected to two neighboring Zr_6 clusters along the *c*-axis (Figure 1c & 1g). Accordingly, two geometrically equivalent linear dicarboxylate ligands, *i.e.* H_2 MPDC (2,5-dicarboxy-1-methylpyridin-1-ium) and H_3 SBDC (2-sulfoterephthalic acid), were selected to install into PCN-700 to form positively and negatively charged microporous MOFs.

As-synthesized single crystals of PCN-700 were

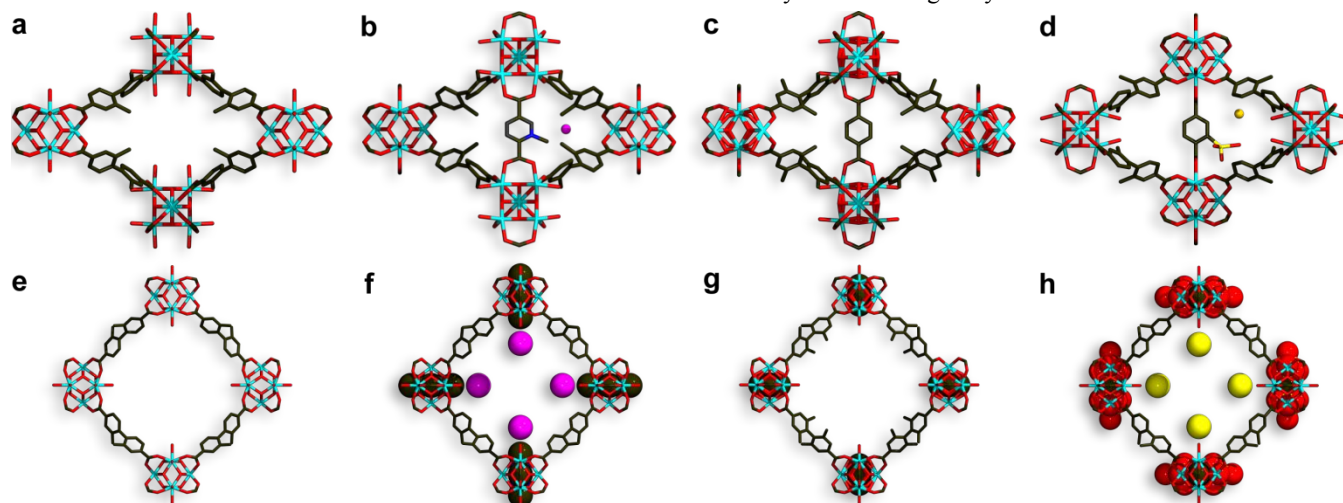


Figure 1. Structures of (a) PCN-700, (b) PCN-700-MPDC, and (c) PCN-700-BDC viewed along the *a*-axes. (d) Structure of PCN-700-SBDC viewed along the *b*-axis. The square 1D channels in (e) PCN-700, (f) PCN-700-MPDC, (g) PCN-700-BDC, and (h) PCN-700-SBDC viewed along the *c*-axes. The MPDC⁺ ligand in PCN-700-MPDC and the SBDC³⁻ ligand in PCN-700-SBDC show significant disorder. Only one installed linker is shown in (b) and (d) for clarity. Color scheme: black, C; red, O; dark blue, N; yellow, S; light blue, Zr; pink, I; khaki, Na.

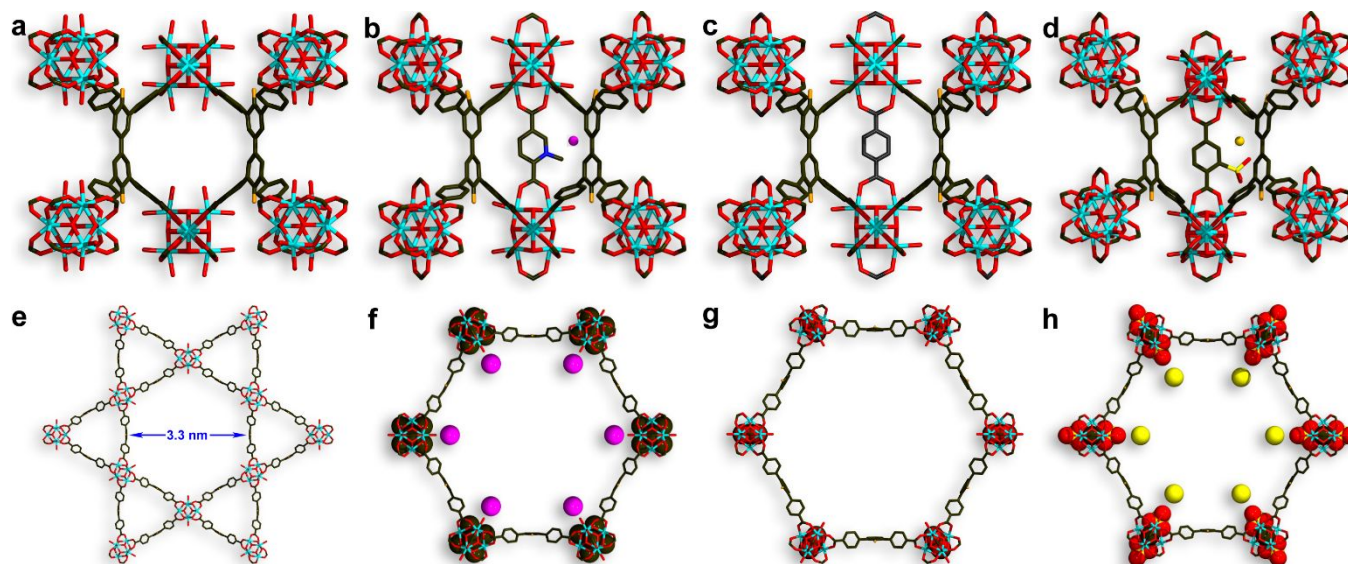


Figure 2. Structure of (a) PCN-608, (b) PCN-608-MPDC, (c) PCN-608-BDC, and PCN-608-SBDC viewed along the (1, 2, 0) direction. The hexagonal 1D channels in (e) PCN-608, (f) PCN-608-MPDC, (g) PCN-608-BDC, and (h) PCN-608-SBDC viewed along the *c*-axes. The MPDC⁻ ligand in PCN-608-MPDC and the SBDC³⁻ ligand in PCN-608-SBDC show significant disorder. Only one installed linker is shown in (b) and (d) for clarity. Color scheme: black, C; red, O; dark blue, N; yellow, S; light blue, Zr; pink, I; khaki, Na; light orange, substituents on the ligands including -NH₂ or -OMe groups.

immersed in DMF solutions of MPDC or SBDC at 85 °C overnight to give the anionic or cationic MOFs, PCN-700-MPDC or PCN-700-SBDC, respectively. Single crystal X-ray diffraction experiments show that all the ionic MOFs remain in the tetragonal space group $P4_2/mmc$ with the *c*-axes slightly decreased after linker installation. The structure of the ionic PCN-700 is similar to that of PCN-700-BDC and the topologies of the MOF changed from a 8-c **bcu** to a 10-c **bct** network (Figure S9). The methyl group on MPDC and the sulfonic acid group on SBDC are highly disordered because of the high symmetry of the frameworks. As shown in Figure 1, the counterions are located in the square 1D channels along the *c*-axes. Powder X-ray diffraction (PXRD) were measured to check the phase purity of the ionic MOFs (Figure S10). The linker ratios in the ionic PCN-700 derivatives were determined by ¹H NMR measurements of the digested samples (Figure S1 and S2, Table S1). The experimental results are a little higher than those calculated from single crystal data because some of the linear linkers may coordinate to the Zr₆ cluster with only one carboxylate, leaving the other end dangling.

As has been reported previously, the PCN-608 series of MOFs crystallize in the hexagonal space group $P6/mmm$ with 3.3 nm hexagonal 1D open channels along the *c*-axis (Figure 2a and 2e). Each Zr₆ cluster in PCN-608 connects to eight fully deprotonated TPCB⁴⁺ fragments and, conversely, each TPCB⁴⁺ fragment links to four Zr₆ clusters (Figure S8). Briefly, PCN-608 adopts the {4,8}-c **csq** network if we simplify the ligands as planar 4-connected nodes and the Zr₆ clusters as 8-connected nodes (Figure S9). Firstly, the amino-substituted PCN-608 was chosen due to the high quality of its single crystals. As-synthesized single crystals of PCN-608-NH₂ were immersed into a solution of H₂BDC in DMF at 85 °C for 24 h before being washed three times with fresh DMF. Single crystal X-ray diffraction experiments at 100 K reveal

that the *a*- and *c*-axes of PCN-608-NH₂-BDC (40.97 Å and 14.81 Å, respectively) are slightly different from that of PCN-608-NH₂ (41.05 Å and 14.69 Å, respectively) with the space group remaining unchanged. Careful analysis of the single crystal structure of PCN-608-NH₂-BDC indicate that the BDC²⁻ ligand installed into PCN-608-NH₂ is also connected to two neighboring Zr₆ clusters along the *c*-axis, as expected (Figure 2c and 2g). After linker installation, the Zr₆ cluster in the mesoporous MOF becomes a 10-connected node and the framework PCN-608-NH₂-BDC adopts a rare {4,10}-c network with a topological point symbol of $\{3^2.4^2.5^2\}2\{3^8.4^{16}.5^8.6^{13}\}$ (Figure S9).³⁶ It should be noted that 10-connected Zr₆ cluster or 12-connected Zr₆ cluster should be exist in the as-synthesized PCN-608-NH₂ or PCN-608-NH₂-BDC if we considered the terminal coordinated monocarboxylate (such as benzoate and trifluoroacetate) or BDC ligand as one ‘connection’. However, this mono-coordination mode is not stable, and tends to be removed by solvent washing and activation. Therefore, the Zr₆ clusters are considered as 8-connected nodes in PCN-608-NH₂ and as 10-connected nodes in PCN-608-NH₂-BDC.

Similarly, ionic mesoporous PCN-608 derivatives, PCN-608-NH₂-MPDC and PCN-608-NH₂-SBDC, were also obtained through solvent assisted installation of H₂MPDC and H₃SBDC (Figure 2). The methyl and sulfonic groups on the installed linkers are also seriously disordered because of the high symmetry of the crystals. The counterions in the ionic PCN-608 series MOFs are also located in the open 1D channels along the *c*-axes (Figure 2). The analog of PCN-608-NH₂ with the amino groups replaced by methoxy groups, PCN-608-OMe, is used for ionic linker installation in order to avoid the influence of the active group in future applications (-OMe is omitted from now on for brevity).

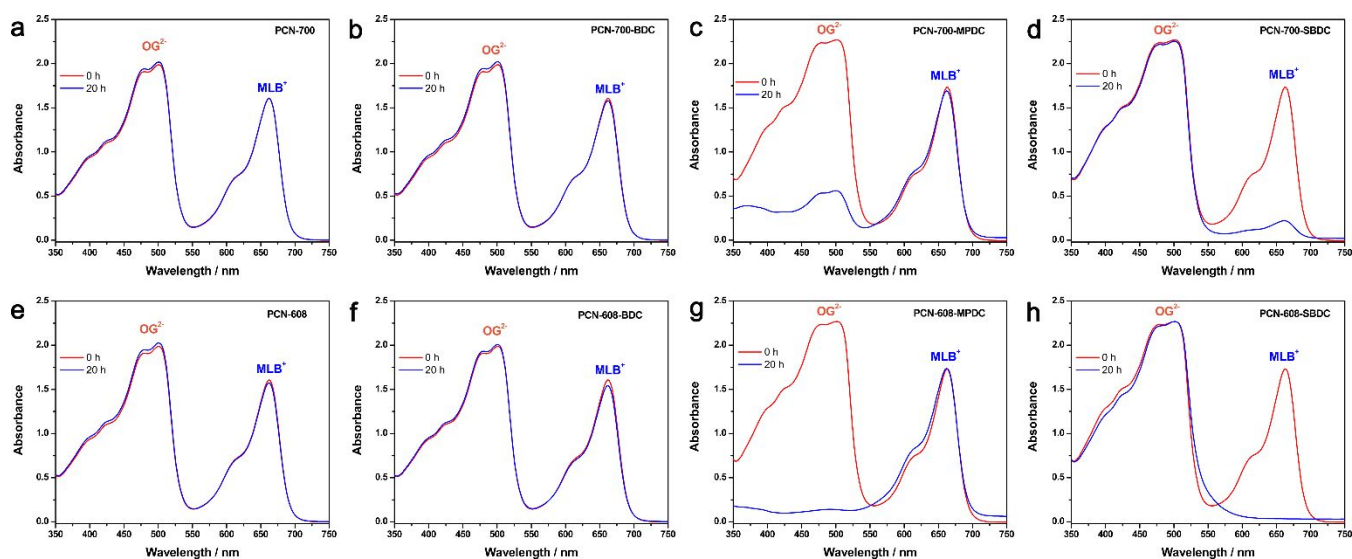


Figure 3. UV-Vis spectra of DMF solutions of $\text{MLB}^+/\text{OG}^{2-}$ in the presence of freshly prepared (a) PCN-700, (b) PCN-700-BDC, (c) PCN-700-MPDC, (d) PCN-700-SBDC, (e) PCN-608, (f) PCN-608-BDC, (g) PCN-608-MPDC, and (h) PCN-608-SBDC. The prototype MOFs PCN-700 and PCN-608, as well as PCN-700-BDC and PCN-608-BDC, which contain the electrically neutral linker BDC, adsorb neither positively nor negatively charged organic dyes. The cationic microporous PCN-700-MPDC and mesoporous PCN-608-MPDC show selective adsorption of the anionic dye OG^{2-} . The anionic microporous PCN-700-SBDC and mesoporous PCN-608-SBDC show selective adsorption of the cationic dye MLB^+ .

Additionally, PXRD patterns were obtained to verify the successful installation of the ditopic linear linkers (Figure S11 and S14). According to powder X-ray diffraction data, the c -axes of PCN-608-BDC, PCN-608-MPDC, and PCN-608-SBDC (14.8063, 15.1671, and 15.0609 Å, respectively) are slightly shortened compared with PCN-608 (15.6163 Å), meaning the installation of the linear dicarboxylate ligands was successful. ^1H NMR spectra of the digested samples were measured in order to figure out the linker ratio in the MOFs (Figure 4c). As shown in Table S1, the linker ratios of the H_4TPCB ligand and the linear dicarboxylate ligands are all approximately 1:1 in PCN-608 derivatives, which is consistent with the calculated results from single crystal data.

It should be noted that the one pot synthesis of PCN-700-MPDC, PCN-700-SBDC, PCN-608-MPDC, and PCN-608-SBDC using a mixture of linkers was not successful. The MPDC ligand is thermally labile and decomposes under solvothermal synthesis. On the other hand, the $-\text{SO}_3^-$ groups tends to coordinate with Zr^{4+} during one-pot reactions to form impurities. DMF was used as solvent during linker installation to facilitate the deprotonation and the subsequent installation of linear linkers. In theory, the process of neutral and ionic linker installation in the zirconium-based MOFs can be accelerated if the proto MOFs were pre-activated to remove the coordinated solvents ($-\text{H}_2\text{O}/\text{OH}^-$), which has been demonstrated in the literature.³⁷⁻⁴⁰ In our specific case, the linker installation can readily occur in as-synthesized MOFs so that the pre-activation was not used.

Selective Ion Exchange by Ionic MOFs. According to the literature, charged MOFs have been considered as platforms for selective, ion-exchange based encapsulation of organic dyes.^{27, 41-43} Therefore, three organic dyes with different

charges, *i.e.* methylene blue (MLB^+), sudan I (SDI^0), and orange G (OG^{2-}) were selected for dye encapsulation in order to verify the charges of the frameworks (Figure S15). It should be noted that the anionic microporous and mesoporous MOF samples were pretreated with dilute NaOH aqueous solution before the ion exchange tests in order to replace the hydrogen ions with sodium ions.

Fresh crystalline samples of PCN-700 and PCN-608 (~10 mg) were put into DMF solutions of MLB^+ , SDI^0 , and OG^{2-} . As expected, the concentrations of all three dyes in DMF solutions were nearly constant after 20 hours, indicating that the prototype MOFs possess electrically neutral frameworks (Figure 3a, 3e, and S16). Additionally, the installation of the uncharged H_2BDC linker into the MOFs has no effect on the chargeability of the prototype frameworks. As shown in Figure S17, the concentrations of all the three kinds of dyes in DMF solutions were nearly constant after fresh crystalline samples of PCN-700-BDC and PCN-608-BDC (~10 mg) were immersed into the solutions for 20 hours. However, when fresh crystalline sample of PCN-700-MPDC and PCN-608-MPDC (~10 mg) were immersed into the solutions for 20 hours, the concentrations of the anionic dye (OG^{2-}) were reduced to almost zero while the concentrations of the cationic and neutral dyes (MLB^+ and SDI^0) remained nearly constant (Figure S18). In addition, selective capture of OG^{2-} from a mixture solution of $\text{OG}^{2-}/\text{MLB}^+$ was also observed for PCN-700-MPDC and PCN-608-MPDC, indicating the cationic nature of the frameworks after H_2MPDC installation (Figure 3c & 3g). On the contrary, the concentrations of the anionic and neutral dyes (OG^{2-} and SDI^0) were nearly constant while the concentration of the cationic dye (MLB^+) was almost reduced to zero after fresh crystalline samples

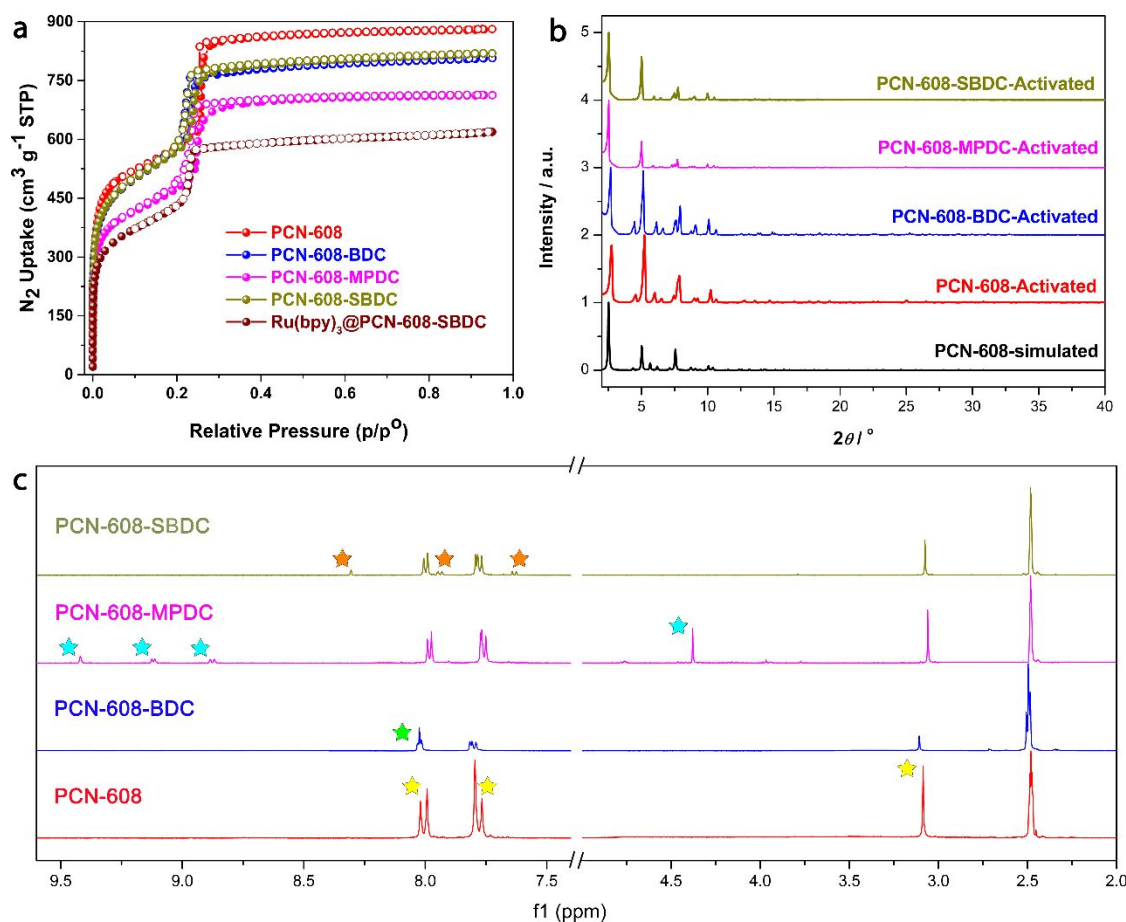


Figure 4. (a) N₂ adsorption isotherms of PCN-608 and its derivatives show typical type IV isotherm shapes. (b) PXRD patterns of PCN-608 and its derivatives after gas adsorption. (c) ¹H NMR spectra of the digested samples for PCN-608 and its derivatives after gas adsorption. The peaks marked with yellow asterisks should be attributed to the main ligand H₄TPCB; part of the green asterisk marked peak should be attributed to the neutral linear linker H₂BDC; the light blue asterisk marked peaks should be attributed to the positively charged linear linker H₂MPDC; and the orange asterisk marked peaks should be attributed to the negatively charged linear linker H₂SBDC.

of PCN-700-SBDC and PCN-608-SBDC (~10 mg) were immersed into the solutions for 20 hours (Figure S19). Moreover, selectively capture of MLB⁺ from a mixture solution of OG²⁻/MLB⁺ was also observed for PCN-700-SBDC and PCN-608-SBDC, indicating the anionic nature of the frameworks after H₃SBDC installation (Figure 3d & 3h).

Porosity Analysis and Stability Tests The N₂ adsorption isotherms were measured for PCN-608 and its derivatives in order to investigate the influence of linker installation on MOF porosity (Figure 4a). Although the saturated N₂ uptake amount decrease significantly after linker installation, all four adsorption isotherms belong to the typical IV isotherm type, indicating the mesoporous nature of the MOFs. The N₂ adsorption amount of PCN-608-SBDC is similar to that of PCN-608-BDC, which may be because some BDC ligands are encapsulated in the pores. Pore size distribution of PCN-608 and its derivatives were also analyzed by NLDFT methods based on the N₂ sorption data, indicating the mesoporosity of the four MOFs (Figure S20). The BET surface areas and pore volumes of the MOFs decrease after neutral and ionic linker installation, while the pore size distributions shift slightly (Table S2). In short, mesopores can survive in the PCN-608 series MOFs after installation of neutral or ionic linkers. ¹H NMR spectra of the digested samples after gas adsorption were measured, showing the integrity of the multicomponent

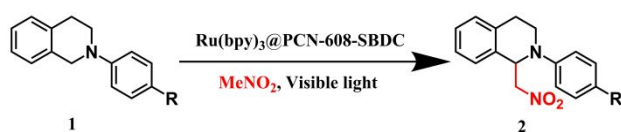
MOFs after activation under high vacuum (Figure 4c). Furthermore, TGA curves of MOF samples before and after insertion of linkers were monitored (Figure S23). The weight loss before 300 °C was attributed to the removal of coordinated water or terminal ligands on the Zr₆ cluster. PCN-608-BDC shows reduced water loss, which is in line with the replacement of terminal H₂O/OH⁻ by BDC linker. PCN-608-SBDC gradually loss water at a lower temperature (before 200 °C), which can be attributed to the removal of Na⁺ coordinated water in the cavity. The methylpyridinium moieties in PCN-608-MPDC are thermally labile, which decomposes at much lower temperature (before 150 °C) compared with other samples.

Immobilization of Cationic Ru(bpy)₃²⁺ Catalysts in Anionic PCN-608-SBDC. Ru(bpy)₃²⁺ has received much attention because of its distinct photocatalytic properties.⁴⁴⁻⁴⁶ Commonly used Ru(bpy)₃²⁺ contains Cl⁻ or PF₆⁻ as counterions.⁴⁷ These kind of photocatalysts show high activity under both UV and visible light. However, the recyclability of this expensive compound is not easy due to its exceptional solubility in commonly used solvents. Considering the coexistence of mesopores and ionic framework in PCN-608 series MOFs, the anionic mesoporous MOF PCN-608-SBDC was chosen to encapsulate Ru(bpy)₃²⁺ cations. In this way, the photocatalyst can be accessed by substrate in the mesopores

and the photocatalyst can be retained inside of the pores and further reused after the product is separated.

As-synthesized PCN-608-SBDC was immersed into an aqueous solution of Ru(bpy)₃Cl₂ after pretreatment with dilute NaOH solution. The cation exchange based Ru(bpy)₃²⁺ adsorption was monitored by UV-Vis spectra (Figure S21). The Ru(bpy)₃²⁺ adsorption amount in PCN-608-SBDC is about 16 mg / 100 mg after 48 hours, which is consistent with the theoretical results from single crystal data supposing each two sodium ions exchange with one Ru(bpy)₃²⁺ ion. The photocatalytic activity of the hybrid Ru(bpy)₃@PCN-608-SBDC was tested by an aza-Henry reaction as a model reaction under visible light. As shown in Table 1, the chloride salt Ru(bpy)₃Cl₂ shows very high conversion yield for the aza-Henry reaction, which is consistent with that of previous reports. However, the catalyst dissolves in the nitromethane solvent and could not be recycled by centrifugation.

Table 1. Aza-Henry reactions catalyzed by the hybrid photocatalyst Ru(bpy)₃@PCN-608-SBDC



catalyst	substrate ^a	conversion yields (%) ^b		
		run 1	run 2	run 3
Ru(bpy) ₃ Cl ₂	1a	99	N.A.	N.A.
PCN-608	1a	18	N.A.	N.A.
PCN-608-SBDC	1a	17	N.A.	N.A.
Ru(bpy) ₃ @PCN-608-SBDC	1a	98	99	93
	1b	98	97	96
	1c	97	98	93

^a For the substrate and the product, 1a, 2a, R = H; 1b, 2b, R = Br; 1c, 2c, R = OCH₃. ^b Conversion yields were determined by ¹H NMR of the crude product.

The conversion yield of the aza-Henry reaction catalyzed by the hybrid photocatalyst was almost as high as that of the chloride salt, when the Ru(bpy)₃²⁺ cation was encapsulated into the mesopores of the anionic PCN-608-SBDC. Three substrates with different substituents were applied in the photocatalytic reaction in order to investigate the wide applicability of the new catalyst. The catalytic activities of Ru(bpy)₃@PCN-608-SBDC for the three substrates are all very high (Table 1). Moreover, the catalyst has been tested for three cycles without an obvious decrease in the conversion yield, indicating that Ru(bpy)₃@PCN-608-SBDC is a promising reusable photocatalyst. Additionally, taking the substrate 1b as an example, catalytic conversion was monitored as a function of time (Figure S24). The conversion steadily increases within 1 hour and then level off. Furthermore, powder X-ray diffraction patterns of the hybrid photocatalyst were measured after three cycles of catalytic reactions, corroborating the stability of the material (Figure S22).

CONCLUSIONS

In conclusion, a series of microporous and mesoporous ionic MOFs has been obtained through installation of ionic

linkers into two prudently selected prototype frameworks (PCN-700 and PCN-608). The topologies of the parent MOFs changed due to the increase in connection number of the Zr₆ cluster from 8-c to 10-c, while the porosity of the networks was retained. Selective ion exchange-based dye capture shows the ionicity of the MOFs. Ru(bpy)₃²⁺ cations can be encapsulated into the anionic mesoporous PCN-608-SBDC and the resulting hybrid photocatalyst shows high catalytic activity and recyclability. Our research sheds light on the design and synthesis of ionic MOFs, as well as the precise regulation of pore environments in both microporous and mesoporous MOFs.

ASSOCIATED CONTENT

Supporting Information.

The Supporting Information is available free of charge via the Internet at <http://pubs.acs.org>.

Text, tables, and figures giving experimental procedures for the syntheses of the ligands, PXRD, N₂ adsorption isotherms, ¹H NMR spectra, and other additional information (PDF)

X-ray crystallographic details of the structures (CIF)

AUTHOR INFORMATION

Corresponding Author

*y dq@fjirsm.ac.cn

*zhou@chem.tamu.edu

Author Contributions

#J.P. and S.Y. contributed equally.

Notes

The authors declare no competing financial interest.

ACKNOWLEDGMENT

The gas sorption studies were supported by the Center for Gas Separations Relevant to Clean Energy Technologies, an Energy Frontier Research Center funded by the U.S. Department of Energy, Office of Science, Office of Basic Energy Sciences (DE-SC0001015). Structural analyses were supported by the Robert A. Welch Foundation through a Welch Endowed Chair to HJZ (A-0030). The National Science Foundation Graduate Research Fellowship (DGE: 1252521) is gratefully acknowledged. The authors also acknowledge the financial support of the U.S. Department of Energy Office of Fossil Energy National Energy Technology Laboratory (DEFE0026472) and National Science Foundation Small Business Innovation Research (NSF-SBIR) program under Grant No. (1632486). The authors also acknowledge the financial supports of the Key Research Program of Frontier Sciences of the Chinese Academy of Sciences (QYZDB-SSW-SLH019 and QYZDY-SSW-SLH025), 973 Program (2014CB932101 and 2013CB933200), National Nature Science Foundation of China (21771177, 21390392 and 21371169), Youth Innovation Promotion Association CAS, and Chun Miao Project of Haixi Institutes (CMZX-2016-001). The powder diffractions were carried out at the Advanced Photon Source on beamline 17-BM-B with the kind assistance of Andrey Yakovenko. S. Yuan also acknowledges the Dow Chemical Graduate Fellowship.

REFERENCES

- Wang, C.; Liu, D.; Lin, W., Metal-organic frameworks as a tunable platform for designing functional molecular materials. *J. Am. Chem. Soc.* **2013**, *135* (36), 13222-13234.
- Lu, W.; Wei, Z.; Gu, Z. Y.; Liu, T. F.; Park, J.; Park, J.; Tian, J.; Zhang, M.; Zhang, Q.; Gentle, T., 3rd; Bosch, M.; Zhou, H. C.,

Tuning the structure and function of metal-organic frameworks via linker design. *Chem. Soc. Rev.* **2014**, *43* (16), 5561-5593.

(3). Schoedel, A.; Li, M.; Li, D.; O'Keeffe, M.; Yaghi, O. M., Structures of Metal-Organic Frameworks with Rod Secondary Building Units. *Chem. Rev.* **2016**, *116* (19), 12466-12535.

(4). Cui, Y.; Li, B.; He, H.; Zhou, W.; Chen, B.; Qian, G., Metal-Organic Frameworks as Platforms for Functional Materials. *Acc. Chem. Res.* **2016**, *49* (3), 483-493.

(5). Furukawa, H.; Cordova, K. E.; O'Keeffe, M.; Yaghi, O. M., The chemistry and applications of metal-organic frameworks. *Science* **2013**, *341* (6149), 1230444.

(6). Trickett, C. A.; Helal, A.; Al-Maythaly, B. A.; Yamani, Z. H.; Cordova, K. E.; Yaghi, O. M., The chemistry of metal-organic frameworks for CO₂ capture, regeneration and conversion. *Nat. Rev. Mater.* **2017**, *2* (8), 17045.

(7). Yang, Q.; Xu, Q.; Jiang, H. L., Metal-organic frameworks meet metal nanoparticles: synergistic effect for enhanced catalysis. *Chem. Soc. Rev.* **2017**, *46* (15), 4774-4808.

(8). Zhou, J.; Wang, B., Emerging crystalline porous materials as a multifunctional platform for electrochemical energy storage. *Chem. Soc. Rev.* **2017**, *46* (22), 6927-6945.

(9). Zhu, L.; Liu, X. Q.; Jiang, H. L.; Sun, L. B., Metal-Organic Frameworks for Heterogeneous Basic Catalysis. *Chem. Rev.* **2017**, *117* (12), 8129-8176.

(10). Bernales, V.; Ortuno, M. A.; Truhlar, D. G.; Cramer, C. J.; Gagliardi, L., Computational Design of Functionalized Metal-Organic Framework Nodes for Catalysis. *ACS Cent. Sci.* **2018**, *4* (1), 5-19.

(11). He, Y.; Chen, F.; Li, B.; Qian, G.; Zhou, W.; Chen, B., Porous metal-organic frameworks for fuel storage. *Coord. Chem. Rev.* **2018**, *373*, 167-198.

(12). Li, J.; Wang, X.; Zhao, G.; Chen, C.; Chai, Z.; Alsaedi, A.; Hayat, T.; Wang, X., Metal-organic framework-based materials: superior adsorbents for the capture of toxic and radioactive metal ions. *Chem. Soc. Rev.* **2018**, *47* (7), 2322-2356.

(13). Lollar, C. T.; Qin, J. S.; Pang, J.; Yuan, S.; Becker, B.; Zhou, H. C., Interior Decoration of Stable Metal-Organic Frameworks. *Langmuir* **2018**, *34* (46), 13795-13807.

(14). Wang, H.; Lustig, W. P.; Li, J., Sensing and capture of toxic and hazardous gases and vapors by metal-organic frameworks. *Chem. Soc. Rev.* **2018**, *47* (13), 4729-4756.

(15). Wen, Y.; Zhang, J.; Xu, Q.; Wu, X.-T.; Zhu, Q.-L., Pore surface engineering of metal-organic frameworks for heterogeneous catalysis. *Coord. Chem. Rev.* **2018**, *376*, 248-276.

(16). Yuan, S.; Feng, L.; Wang, K.; Pang, J.; Bosch, M.; Lollar, C.; Sun, Y.; Qin, J.; Yang, X.; Zhang, P.; Wang, Q.; Zou, L.; Zhang, Y.; Zhang, L.; Fang, Y.; Li, J.; Zhou, H. C., Stable Metal-Organic Frameworks: Design, Synthesis, and Applications. *Adv. Mater.* **2018**, *30* (37), e1704303.

(17). Zhao, X.; Wang, Y.; Li, D. S.; Bu, X.; Feng, P., Metal-Organic Frameworks for Separation. *Adv. Mater.* **2018**, *30* (37), e1705189.

(18). Karmakar, A.; Desai, A. V.; Ghosh, S. K., Ionic metal-organic frameworks (iMOFs): Design principles and applications. *Coord. Chem. Rev.* **2016**, *307*, 313-341.

(19). He, H.; Hashemi, L.; Hu, M.-L.; Morsali, A., The role of the counter-ion in metal-organic frameworks' chemistry and applications. *Coord. Chem. Rev.* **2018**, *376*, 319-347.

(20). Li, Y.; Yang, Z.; Wang, Y.; Bai, Z.; Zheng, T.; Dai, X.; Liu, S.; Gui, D.; Liu, W.; Chen, M.; Chen, L.; Diwu, J.; Zhu, L.; Zhou, R.; Chai, Z.; Albrecht-Schmitt, T. E.; Wang, S., A mesoporous cationic thorium-organic framework that rapidly traps anionic persistent organic pollutants. *Nat. Commun.* **2017**, *8* (1), 1354.

(21). Johnson, J. A.; Petersen, B. M.; Kormos, A.; Echeverria, E.; Chen, Y. S.; Zhang, J., A New Approach to Non-Coordinating Anions: Lewis Acid Enhancement of Porphyrin Metal Centers in a Zwitterionic Metal-Organic Framework. *J. Am. Chem. Soc.* **2016**, *138* (32), 10293-8.

(22). Li, P.; Vermeulen, N. A.; Gong, X.; Malliakas, C. D.; Stoddart, J. F.; Hupp, J. T.; Farha, O. K., Design and Synthesis of a Water-Stable Anionic Uranium-Based Metal-Organic Framework

(MOF) with Ultra Large Pores. *Angew. Chem. Int. Ed.* **2016**, *55* (35), 10358-10362.

(23). Desai, A. V.; Manna, B.; Karmakar, A.; Sahu, A.; Ghosh, S. K., A Water-Stable Cationic Metal-Organic Framework as a Dual Adsorbent of Oxoanion Pollutants. *Angew. Chem. Int. Ed.* **2016**, *55* (27), 7811-7815.

(24). Gao, Q.; Xu, J.; Cao, D.; Chang, Z.; Bu, X. H., A Rigid Nested Metal-Organic Framework Featuring a Thermoresponsive Gating Effect Dominated by Counterions. *Angew. Chem. Int. Ed.* **2016**, *55* (48), 15027-15030.

(25). Zhao, X.; Bu, X.; Zhai, Q. G.; Tran, H.; Feng, P., Pore space partition by symmetry-matching regulated ligand insertion and dramatic tuning on carbon dioxide uptake. *J. Am. Chem. Soc.* **2015**, *137* (4), 1396-1399.

(26). Zhao, X.; Bu, X.; Nguyen, E. T.; Zhai, Q. G.; Mao, C.; Feng, P., Multivariable Modular Design of Pore Space Partition. *J. Am. Chem. Soc.* **2016**, *138* (46), 15102-15105.

(27). Zhao, X.; Mao, C.; Luong, K. T.; Lin, Q.; Zhai, Q. G.; Feng, P.; Bu, X., Framework Cationization by Preemptive Coordination of Open Metal Sites for Anion-Exchange Encapsulation of Nucleotides and Coenzymes. *Angew. Chem. Int. Ed.* **2016**, *55* (8), 2768-2772.

(28). Oisaki, K.; Li, Q.; Furukawa, H.; Czaja, A. U.; Yaghi, O. M., A metal-organic framework with covalently bound organometallic complexes. *J. Am. Chem. Soc.* **2010**, *132* (27), 9262-9264.

(29). Brozek, C. K.; Dinca, M., Cation exchange at the secondary building units of metal-organic frameworks. *Chem. Soc. Rev.* **2014**, *43* (16), 5456-5467.

(30). Yuan, S.; Chen, Y. P.; Qin, J. S.; Lu, W.; Zou, L.; Zhang, Q.; Wang, X.; Sun, X.; Zhou, H. C., Linker Installation: Engineering Pore Environment with Precisely Placed Functionalities in Zirconium MOFs. *J. Am. Chem. Soc.* **2016**, *138* (28), 8912-8919.

(31). Yuan, S.; Lu, W.; Chen, Y. P.; Zhang, Q.; Liu, T. F.; Feng, D.; Wang, X.; Qin, J.; Zhou, H. C., Sequential linker installation: precise placement of functional groups in multivariate metal-organic frameworks. *J. Am. Chem. Soc.* **2015**, *137* (9), 3177-3180.

(32). Qin, J. S.; Yuan, S.; Alsalmeh, A.; Zhou, H. C., Flexible Zirconium MOF as the Crystalline Sponge for Coordinative Alignment of Dicarboxylates. *ACS Appl. Mater. Interfaces* **2017**, *9* (39), 33408-33412.

(33). Pang, J.; Yuan, S.; Qin, J.; Wu, M.; Lollar, C. T.; Li, J.; Huang, N.; Li, B.; Zhang, P.; Zhou, H. C., Enhancing Pore-Environment Complexity Using a Trapezoidal Linker: Toward Stepwise Assembly of Multivariate Quinary Metal-Organic Frameworks. *J. Am. Chem. Soc.* **2018**, *140* (39), 12328-12332.

(34). Pang, J.; Yuan, S.; Du, D.; Lollar, C.; Zhang, L.; Wu, M.; Yuan, D.; Zhou, H. C.; Hong, M., Flexible Zirconium MOFs as Bromine-Nanocontainers for Bromination Reactions under Ambient Conditions. *Angew. Chem. Int. Ed.* **2017**, *56* (46), 14622-14626.

(35). Pang, J.; Yuan, S.; Qin, J.; Liu, C.; Lollar, C.; Wu, M.; Yuan, D.; Zhou, H. C.; Hong, M., Control the Structure of Zr-Tetracarboxylate Frameworks through Steric Tuning. *J. Am. Chem. Soc.* **2017**, *139* (46), 16939-16945.

(36). Blatov, V. A.; Shevchenko, A. P.; Proserpio, D. M., Applied Topological Analysis of Crystal Structures with the Program Package ToposPro. *Cryst. Growth Des.* **2014**, *14* (7), 3576-3586.

(37). Kim, H. K.; Yun, W. S.; Kim, M. B.; Kim, J. Y.; Bae, Y. S.; Lee, J.; Jeong, N. C., A Chemical Route to Activation of Open Metal Sites in the Copper-Based Metal-Organic Framework Materials HKUST-1 and Cu-MOF-2. *J. Am. Chem. Soc.* **2015**, *137* (31), 10009-10015.

(38). Bae, J.; Choi, J. S.; Hwang, S.; Yun, W. S.; Song, D.; Lee, J.; Jeong, N. C., Multiple Coordination Exchanges for Room-Temperature Activation of Open-Metal Sites in Metal-Organic Frameworks. *ACS Appl. Mater. Interfaces* **2017**, *9* (29), 24743-24752.

(39). Bae, J.; Lee, E. J.; Jeong, N. C., Metal coordination and metal activation abilities of commonly unreactive chloromethanes toward metal-organic frameworks. *Chem. Commun.* **2018**, *54* (50), 6458-6471.

(40). Choi, J. S.; Bae, J.; Lee, E. J.; Jeong, N. C., A Chemical Role for Trichloromethane: Room-Temperature Removal of Coordinated

Solvents from Open Metal Sites in the Copper-Based Metal-Organic Frameworks. *Inorg. Chem.* **2018**, *57* (9), 5225-5231.

(41). Yu, J.; Cui, Y.; Xu, H.; Yang, Y.; Wang, Z.; Chen, B.; Qian, G., Confinement of pyridinium hemicyanine dye within an anionic metal-organic framework for two-photon-pumped lasing. *Nat. Commun.* **2013**, *4*, 2719.

(42). Zhao, X.; Bu, X.; Wu, T.; Zheng, S. T.; Wang, L.; Feng, P., Selective anion exchange with nanogated isorecticular positive metal-organic frameworks. *Nat. Commun.* **2013**, *4*, 2344.

(43). Cai, H.; Li, M.; Lin, X. R.; Chen, W.; Chen, G. H.; Huang, X. C.; Li, D., Spatial, Hysteretic, and Adaptive Host-Guest Chemistry in a Metal-Organic Framework with Open Watson-Crick Sites. *Angew. Chem. Int. Ed.* **2015**, *54* (36), 10454-10459.

(44). Drolen, C.; Conklin, E.; Hetterich, S. J.; Krishnamurthy, A.; Andrade, G. A.; Dimeglio, J. L.; Martin, M. I.; Tran, L. K.; Yap, G. P. A.; Rosenthal, J.; Young, E. R., pH-Driven Mechanistic Switching from Electron Transfer to Energy Transfer between [Ru(bpy)₃]²⁺ and Ferrocene Derivatives. *J. Am. Chem. Soc.* **2018**, *140* (32), 10169-10178.

(45). Li, G.; Brady, M. D.; Meyer, G. J., Visible Light Driven Bromide Oxidation and Ligand Substitution Photochemistry of a Ru Diimine Complex. *J. Am. Chem. Soc.* **2018**, *140* (16), 5447-5456.

(46). Wang, C.; Xie, Z.; deKrafft, K. E.; Lin, W., Doping metal-organic frameworks for water oxidation, carbon dioxide reduction, and organic photocatalysis. *J. Am. Chem. Soc.* **2011**, *133* (34), 13445-13454.

(47). Dai, C.; Narayanam, J. M.; Stephenson, C. R., Visible-light-mediated conversion of alcohols to halides. *Nat. Chem.* **2011**, *3* (2), 140-145.

